PCCP

PAPER

Characterisation of the electronic structure of some stable nitroxyl radicals using variable energy photoelectron spectroscopy

Cite this: *Phys. Chem. Chem. Phys.*, 2014, **16**, 10734

Branka Kovač,[a] Ivan Ljubić,*[a] Antti Kivimäki,[b] Marcello Coreno[c] and Igor Novak*[d]

Received 27th February 2014,
Accepted 1st April 2014

DOI: 10.1039/c4cp00867g

www.rsc.org/pccp

The photoionization of three stable nitroxyl radicals has been studied in the valence and core regions using synchrotron radiation. We observed different variations of the relative band intensities with the photon energy for two pyrrolidine nitroxyls (nitroxyl8 and nitroxyl9) in the valence ionization region. This is due to strong intramolecular interactions between the amide substituent and the ring π-orbital when present. In the core ionization region we observed chemical shifts which were consistent with the relative electron affinities of different atoms. We also observed the multiplet splitting of core level binding energies in the final ionic states. The core electron binding energies calculated *via* the restricted open shell Hartree–Fock based ΔSCF method exhibit good agreement with the experimental core ionization bands and with the assignment of the spectra by empirical analysis.

Introduction

Stable nitroxyl radicals (SNR) represent a very important class of compounds with applications in synthetic chemistry (polymerization catalysts), as precursors for organic ferromagnetic materials and as spin labels especially in biochemical studies.[1] The electronic structure is the crucial factor which governs the properties of SNR and consequently underpins their applications and has been studied with fixed photon energy sources in the valence and core photoionization regions.[2,3] In this work we present a study of the electronic structures of the piperidine nitroxyl radical TEMPO and two pyrrolidine nitroxyl radicals nitroxyl8 and nitroxyl9 (Fig. 1; the labelling for the latter two compounds follows that of ref. 2), using photoelectron spectroscopy with a tuneable radiation source (synchrotron). The X-ray photoelectron spectroscopy (XPS) and ultraviolet photoelectron spectroscopy (UPS) methods provide different types of information; while UPS results can be useful for *e.g.* studying the adsorption of free radicals on metallic surfaces, XPS results can be useful for analyzing the electron and spin density distributions in free and metal-coordinated radicals.[3] Small open shell systems like NO and O_2 have been studied previously,[4] but to the best of our knowledge the results presented here represent the first reported XPS spectra of larger open shell polyatomics in the gas phase.

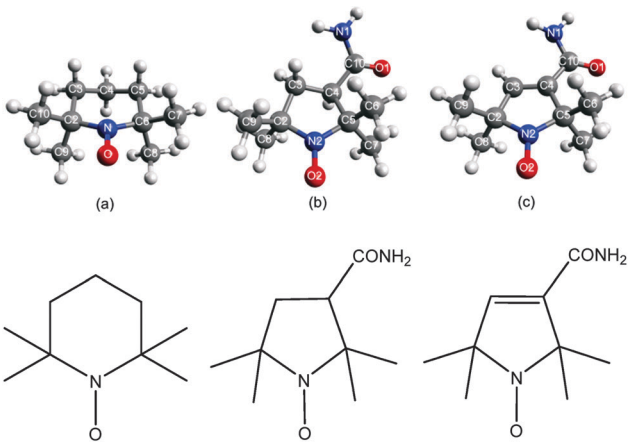

Fig. 1 Structures and labeling of the atoms of the three studied nitroxyl radicals: (a) TEMPO (C_s symmetry) (b) nitroxyl8 and (c) nitroxyl9.

The XPS peaks will yield core electron binding energies (CEBEs) of the C, N, and O atoms, which will be used to test the performance of the restricted open shell Hartree–Fock (ROHF) based ΔSCF method for calculating those energies.[5] The ΔSCF method, albeit one based on the unrestricted HF formalism, has recently been shown to provide an accurate and efficient approach to computing core excited states.[6] Assessing the performance of the ROHF ΔSCF in the examples of the ground state open shell systems appears not to have been reported before, yet it is important because such systems traditionally pose major difficulties to quantum chemical

[a] *Ruđer Bošković Institute, Bijenička cesta 54, HR-10000 Zagreb, Croatia. E-mail: iljubic@irb.hr*
[b] *CNR-IOM, Laboratorio Nazionale TASC, 34149 Trieste, Italy*
[c] *CNR-IMIP, Montelibretti, 00016 Rome, Italy*
[d] *Charles Sturt University, POB 883, Orange, NSW 2800, Australia. E-mail: inovak@csu.edu.au*

treatments and are in particular expected to benefit more from the requirement on the total spin to be a good quantum number.

Experimental and computational methods

The samples of the compounds studied in this work were obtained from Sigma-Aldrich. The identity and purity of samples was checked by NMR and GC measurements. The UV and X-ray photoelectron spectra were measured at the Gas Phase Photoemission beam line of the synchrotron radiation facility Elettra, Trieste (Italy), using a commercial six-channel, 150 mm hemispherical electron energy analyser (VG i220) installed at the magic angle (54.7°) with respect to (horizontal) linearly polarized light.[7] Therefore the measurements are insensitive to the variation of the photoelectron asymmetry parameter β. For valence ionizations a wide range of ionization energies from 15 eV to 70 eV (with 5–10 eV photon energy intervals) were used in order to capture the important spectral features. The C1s, N1s and O1s photoelectron spectra were recorded at photon energies of 382, 495 and 628 eV, respectively, *i.e.* the photon energies were approximately 90 eV above the respective core ionization thresholds so that post-collision interaction effects could be neglected. The photon energy resolutions were approximately 150 meV (70 meV) at 382 eV photon energy, 150 meV (120 meV) at 495 eV photon energy and 250 meV (220 meV) at 628 eV photon energy for nitroxyl8 and nitroxyl9 (and for TEMPO). The C1s, N1s and O1s binding energies of the compounds studied here were calibrated by measuring their XPS spectra together with CO_2 (C1s at 297.6 eV, O1s at 541.3 eV) and N_2 (N1s at 409.9 eV).[8] The kinetic energy resolution of the analyzer was about 2% of the pass energy used. Valence band spectra were measured at 5 eV pass energy, while the core photoemission spectra were recorded at 10 and 7 eV pass energies (for nitroxyl8/9 and TEMPO, respectively).

The CEBE of the C, N, and O atoms of the three nitroxyl radicals (Fig. 1) were calculated using the ROHF based ΔSCF method, *i.e.* as the energy difference between the SCF converged ROHF wave functions of the ground (doublet) and the core–hole (triplet) state of the radicals. Only the triplet multiplicity was considered for the core–hole cations. In line with the previous study on CEBEs of a series of organic compounds,[5] we resorted to the use of mixed basis set in order to alleviate the SCF convergence by ensuring localization of the core–hole exclusively to the center atom of interest. We used the cc-pCVTZ basis set[9] on the atom whose CEBE is calculated in a given run. The presence of the additional core basis functions relative to the more usual cc-pVTZ set is expected to provide a greater flexibility in description of the core region, similarly to the approach of uncontracting the basis sets.[6] On the hydrogen atoms the standard correlation consistent double-zeta basis set was used (cc-pVDZ),[10] while for the remaining C, O, and N atoms the model core potentials (MCP) were used with a double-zeta contraction and a set of *d* polarization functions in the valence space (MCP-dzp) as devised by Miyoshi and co-workers.[11] Such a mixed basis set simplifies the calculations significantly because it gives rise to only one core orbital which is fixed to the atom center of interest.[13] The collapse of the core–hole states was prevented by restricting the orbital mixing (interchanges) during the SCF procedure and switching on the Pulay's DIIS convergence accelerator[12] instead of the second-order SCF. Even so, in the majority of cases the course of the SCF convergence was erratic and very cumbersome, and the SCF procedure had to be restarted several times, each time supplying a slightly better initial density guess. The relativistic corrections are presently neglected but for the UHF based ΔSCF and the here relevant C, N, and O atoms these were estimated to raise the CEBEs by 0.1 to 0.4 eV.[6] The ΔSCF CEBEs were calculated for the geometries of the radicals optimized at the U-B3LYP/6-31+G(d) level. The GAMESS-US quantum chemical suite was used.[13]

Results and discussion

Valence ionizations

The photoelectron (PE) spectra corresponding to valence ionizations of nitroxyl8 and nitrroxyl9 were recorded in the 15–70 eV photon energy range (Fig. 2 and 3). Our PE spectra are consistent with HeI/HeII spectra reported previously.[2] Only electron emission from the HOMO, corresponding to the first band (X) in the spectrum appears well resolved, whereas the subsequent four bands (A–D) at higher ionization energies are only partially resolved. A–D bands correspond to ionizations from the oxygen lone pair located at the nitroxyl group [n_{NO} (triplet), n_{NO} (singlet)] and the lone pairs (n_{CO}, n_{NH_2}) from the amide group. Above the ionization energy of 11 eV the density

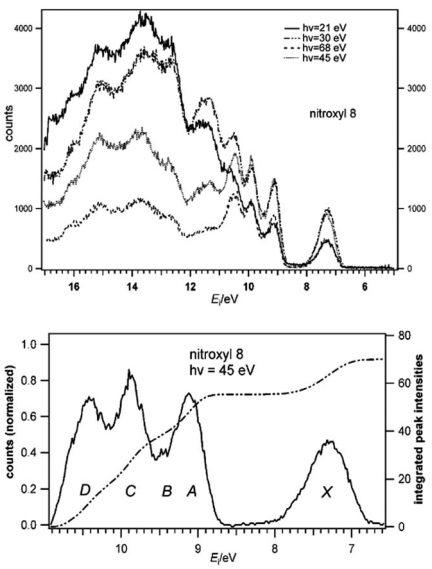

Fig. 2 UV photoelectron spectra of nitroxyl8 measured at different photon energies (top panel). In the bottom panel, the dashed-dotted line gives the integrated spectral intensity in the displayed region. The spectrum measured at $h\nu$ = 45 eV is shown as an example. The intensity was normalized by dividing by the max value and the baseline for subtraction was fitted using a sum of two exponentially decaying functions and a constant.

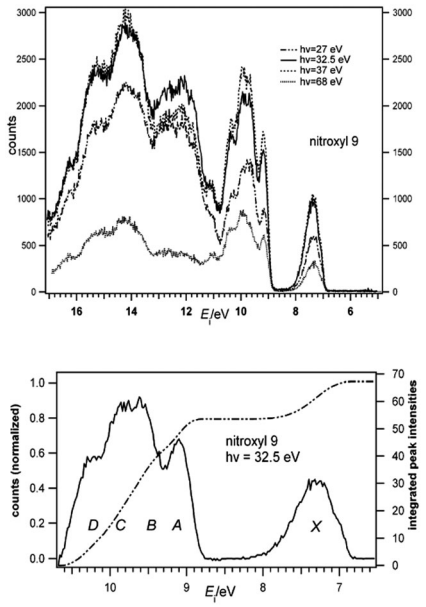

Fig. 3 UV photoelectron spectra of nitroxyl9 measured at different photon energies (top panel). In the bottom panel, the dashed-dotted line gives the integrated spectral intensity in the displayed region. The spectrum measured at $h\nu$ = 32.5 eV is shown as an example. The intensity was normalized by dividing by the max value and the baseline for subtraction was fitted using a sum of two exponentially decaying functions and a constant.

of the ionic states becomes very large, and the spectrum consists of many broad and overlapping photoemission bands.

Our principal interest is focused on band intensities corresponding to photoemission from different ionic states as a function of photon energy. Thus we have concentrated on spectral features below 11 eV ionization energy, which are better resolved and can be reliably assigned.[2]

We have extracted from the PE spectra the integrated intensity of the HOMO and of the A–D bands and we have plotted the ratio X/(A + B + C + D) as a function of photoelectron kinetic energy in Fig. 4.

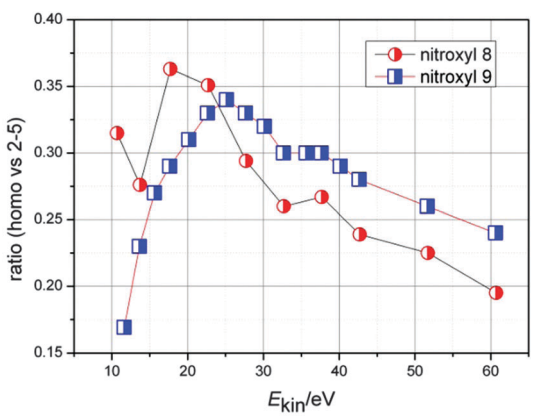

Fig. 4 Variation of the relative band intensities of valence ionizations for nitroxyl8 and nitroxyl9 as a function of the photoelectron kinetic energy. The ratio (homo *vs.* 2–5) represents the ratio of intensity of the X ionization band *vs.* the total intensity of the subsequent four ionization bands A–D at a given photoelectron energy.

Table 1 Bond lengths/Å of amide group moiety in nitroxyl8 and nitroxyl9

	C–C	C–CO	C═O	C–NH_2
Nitroxyl8	1.530	1.517	1.218	1.350
Nitroxyl9	1.319	1.490	1.230	1.329

This approach also circumvented problems with variations of experimental conditions in different scans, deriving from possible longer term drifts in the absolute pressure of the vapor in the interaction region, as well as in synchrotron beam conditions.

This ratio clearly shows that the intensity variations for nitroxyl8 and nitroxyl9 are quite different in the kinetic energy range 10–40 eV. The reason for the discrepancy is not due to the electronic structures of the nitroxyl groups with its unpaired electrons. Rather, the discrepancy is due to different electronic structures of the exocyclic amide group in nitroxyl8 and nitroxyl9. In the former molecule, the amide group is not conjugated to the ring orbitals while in the latter the amide substituent is conjugated to the ring π-orbital. This suggestion is supported by structural data for the two molecules (Table 1).[14] Single bonds comprising the amide group in nitroxyl9 are shorter than in nitroxyl8 while the C═O bond in nitroxyl9 is longer *i.e.* the bond alternation is reduced if conjugation with the ring π-orbital is possible. Measured molecular structures of the two pyrrolidine nitroxyls exhibit no evidence of intramolecular interactions between the nitroxyl and amide moieties as exemplified by the fact that the N–O bond lengths in nitroxyl8 and nitroxyl9 are 1.268 and 1.267 Å, respectively.[14]

A significant difference between the electronic structures of the amide group in nitroxyl8 and nitroxyl9 (induced by π-conjugation in nitroxyl9) is related to the different amide MO compositions which lead to different photoionization cross-sections[15] and hence different variations in the relative band intensity with kinetic energy. Amide orbitals can be expected to have more C2p character in nitroxyl9 than in nitroxyl8. Atomic photoionization cross-sections[15] for C2p, N2p and O2p vary differently with kinetic energy. Therefore, the relative band intensities of the corresponding amide orbitals A + B + C + D in the two nitroxyls will also vary differently with the photoelectron kinetic energy. This information about amide substituent groups could not be derived from the previous UPS study performed at fixed photon energies.[2]

Core ionizations

The assignment of core ionization bands can be achieved by empirical or by computational methods. The empirical method is based on comparison of the observed chemical shifts for given classes of atoms present in different but related molecules. The quantitative assignment requires the use of high-level computational methods. We employed both methods in our work to assign the C1s, N1s and O1s spectra of TEMPO, nitroxyl8 and nitroxyl9. All the spectra have been deconvoluted using a number of Voigt profiles defined by the fixed gaussian contribution (depending on the experimental resolution

(photon and electron analyser resolution)) and lorentzian which is due to the lifetime broadening. The gaussian full width at half maximum (fwhm) thus differs for C1s, N1s and O1s for TEMPO and nitroxyls (see the Experimental part), while the lorentzian fwhm was fixed at 0.16, 0.13 and 0.1 eV for O1s, N1s and C1s respectively, assuming that they are similar to the corresponding lifetime widths in diatomic molecules.[16a] A routine available in IGOR Pro (WaveMatrix Inc.) was used for fitting.

Furthermore, the overall shape of the N1s and O1s bands due to the intensities of vibronic progressions was fitted using the linear coupling model (LCM).[17] The model assumes that Franck–Condon (FC) factors are expressed in terms of the first-order (linear) electron-vibrational coupling constants given by the gradient of the final state potential energy at the initial state equilibrium geometry.[17] The initial and final states are described by identical harmonic potential surfaces (the same force constant k) differing only in their equilibrium geometry. The intensity of a composite vibronic transition is given by the product of Poisson distributions taken over the intensities of the individual symmetry allowed vibronic transitions. For any of them the corresponding FC factor is given by:

$$I(v \leftarrow 0) = \frac{S^v}{v!}\exp(-S) \quad (1)$$

('absolute' intensities), with v being vibrational quantum number. The S factor can be determined from the photoelectron spectrum as the ratio of intensities I(1–0)/I(0–0). If, on the other hand, all one is interested in are ratios of intensities, one simply uses:

$$\frac{I(v \leftarrow 0)}{I(0-0)} = \frac{S^v}{v!} \quad (2)$$

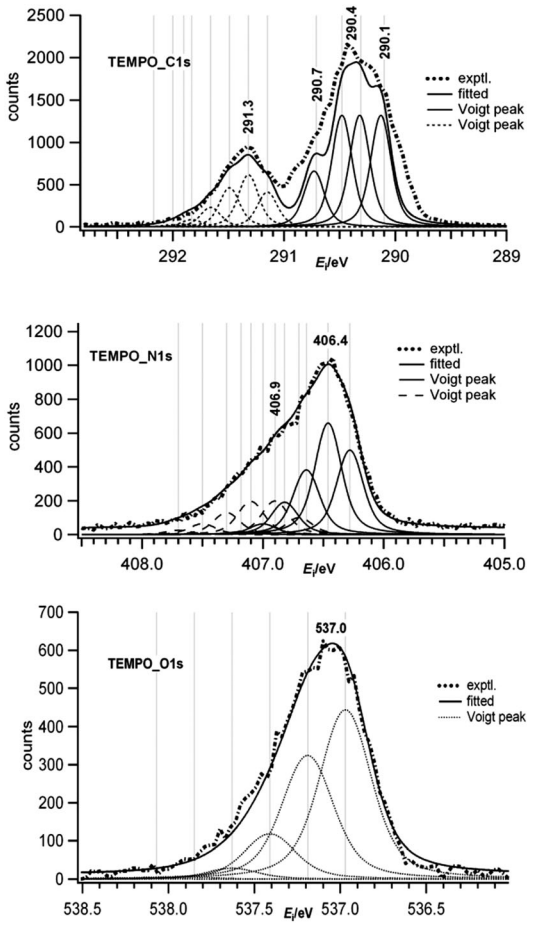

Fig. 5 C1s, N1s and O1s in XPS of the TEMPO radical.

TEMPO

The carbon atom directly bonded to a more electronegative heteroatom (*e.g.* oxygen or nitrogen) is expected to have a higher C1s energy than the carbon attached to other carbons. In TEMPO two bands, a broad one in the range of 289.5–291 eV and another one at 291.3 eV, have the intensity ratio of ~7 : 2 (Fig. 5). This suggests that the 291.3 eV band corresponds to ionization of C1s electrons from carbons which are in the α-position with respect to the nitroxyl group (C2 and C6) while the broad band comprises C1s ionizations from the remaining carbon atoms. Since seven electronic systems occupy a narrow (~1.5 eV) energy range, their deconvolution is a difficult task. Following the predictions of quantum chemical calculations (Table 3) we have only used four Voigt profiles to reproduce the gross features of the intensity distribution, excluding all the vibrational structure. TEMPO belongs to the C_s point group, so we use three Voigt profiles for three by symmetry equivalent types of carbon atoms (C3 = C5, C8 = C9, C7 = C10) and one profile for the C4 atom with the intensity ratio of 2 : 2 : 2 : 1.

The band at 291.3 eV, on the other hand, is assigned to ionization from two equivalent C atoms (C2 = C6), so we assumed that it could be fitted using the linear coupling model. Progression of 0.17 eV and S = 1.5 provided a fairly good agreement with the experimental envelope although the results cannot be regarded as definitive (Fig. 5).

The N1s and O1s ionizations are easy to identify since only a single heteroatom of each type is present in TEMPO. We notice, however, that the N1s band has a more asymmetrical profile than the O1s band. We detect a splitting of 0.5 eV in the N1s band with vertical transitions at 406.4 and 406.9 eV. This multiplet splitting of core-level binding energies is a final ionic state effect which is known to take place in open-shell molecular systems.[4b,c] The splitting is due to electron coupling between the unpaired electron in the N1s core orbital and the unpaired valence electron in the HOMO.[4] The observation of the splitting in the N1s band but not in the O1s band could tentatively be attributed to the known larger population of the unpaired valence electron in the oxygen atom than in the nitrogen atom.[18] The larger spin density of the oxygen atom would reduce the O1s core–hole lifetime (*via* core–valence interactions) and thus increase the O1s bandwidth blurring any multiplet splitting. However, there are additional explanations for why O1s splitting is not observed. The natural line widths of the N1s and O1s ionized states (in diatomics) are 0.13 and 0.16 eV, respectively.[16a] Furthermore, the multiplet splitting may be smaller in O1s ionization than in N1s ionization, as was observed in the NO molecule.[4] Therefore, the multiplet splitting may also be more difficult to observe in the O1s band of TEMPO because the experimental resolution in the O1s

region is lower due to the higher photon energy used. In other words, the splitting in the O1s band could be hidden within the broader spectral profile. Such explanation is supported by deconvolution of N1s and O1s spectra: FC envelopes were fitted with two and one vibrational progression respectively, assuming the validity of the linear coupling model (Fig. 5). Whereas $I(1\text{–}0)$ is of higher intensity than $I(0\text{–}0)$ in N1s indicating the change in the equilibrium geometry during the ionization event, the adiabatic ($I(0\text{–}0)$) transition seems to be the most intense one in O1s. Examples in which the adiabatic transition is not the most intense one, to the best of our knowledge, represent a rather rare case.[19] However, it is not necessary that the vertical transition should be from the lowest to the lowest vibrational state for LCM to remain valid; namely, if the most intense transition is assumed to be ν–0 then only the center of the Poisson distribution in LCM is shifted but the distribution itself still holds and governs the intensities of transitions on the high- and low-energy side of the ν–0 center. Since the spectra are unresolved one can only try to analyse and predict the shape of the vibrational distribution. The vibrational energy of the N–O stretching mode amounts to 1339 cm^{-1} (0.166 eV) in the molecular ground state of TEMPO.[16b] This value suggests that vibronic excitation may cause some broadening in the N1s and O1s bands. Such vibronic broadening could be different in the N1s and O1s ionized states depending on the changes in the respective N–O bond strengths induced by N1s or O1s ionizations. Relaxation of electron orbitals is known to alter the bond lengths and strengths differently in different core ionic states as was shown for C1s and O1s ionizations of carbon monoxide.[20] Convolution of the N1s FC profile is satisfactory if one assumes that $S = 1.32$ and $\nu = 0.18$ eV (full line) and $S = 1.98$ and $\nu = 0.20$ eV (dashed line) (Fig. 5). Similarly, the fitted FC envelope of O1s can be reproduced upon the assumption that only one local mode involving N–O stretching with $\nu = 0.22$ eV ($S = 0.73$) is excited. The fit, however, does not provide a conclusive proof that the other component of the singlet–triplet (S–T) split state would not be populated.

Amide substituted pyrrolidine nitroxyls

We can identify three classes of carbon atoms in their spectra: one amide carbon (C10), two carbons in α-positions *vs.* the nitroxyl group (C2, C5) and the remaining six carbons. The number of atoms in each class stands in the ratio 6 : 2 : 1 in both molecules and corresponds to three resolved bands in the C1s core ionization spectra (Fig. 6 and 7). These bands also have relative intensity ratios ~6 : 2 : 1. These ratios can be used to assign C1s ionization of specific carbon atoms to a particular band (Table 2).

Deconvolution by the right number of Voigt functions (with already mentioned defined analyser and monochromator broadenings) gives the acceptable FC profiles (Fig. 6 and 7) and is also in accord with the quantum chemical results (Table 3). But one has to keep in mind that no vibrational structure has been taken into account, thus the greater deviation from experimental results. Although these molecules do not possess a non-trivial symmetry, calculation results suggest

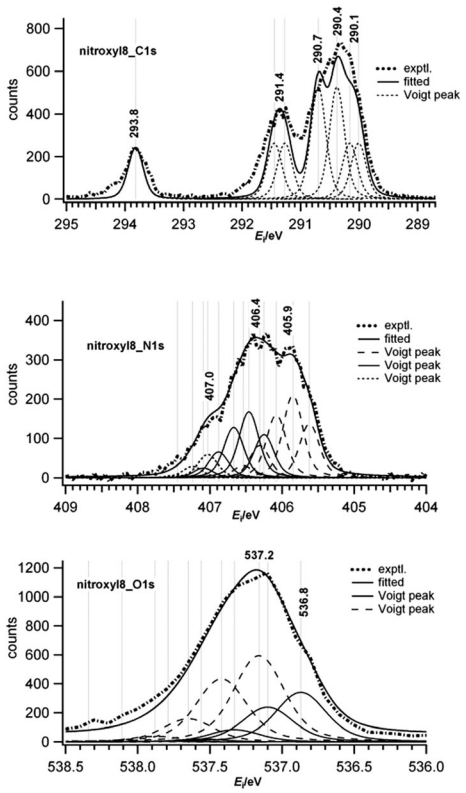

Fig. 6 C1s, N1s, O1s in XPS of the nitroxyl8 radical.

that the core ionization energies of C3, C4 and C8, C9 are almost degenerate in nitroxyl8, and C3, C4 in nitroxyl9. Therefore four Voigt functions with an intensity ratio 2 : 2 : 1 : 1 and five with a ratio 2 : 1 : 1 : 1 : 1 were used for the fitting procedure in nitroxyl8 and nitroxyl9, respectively. An independent check of the assignments can be made by comparing our ionization energies with the results from X-ray photoelectron spectra of amides and related compounds[21] and with our XPS for the unsubstituted TEMPO derivative (Fig. 5). The C1s, N1s and O1s ionization energies in formamide ($HCONH_2$) are 294.56, 406.33 and 537.71 eV, respectively. We have observed that C1s ionization from amide carbon atom (C10) appears at a higher ionization energy in nitroxyl9 than in nitroxyl8. This can be rationalized as follows. The valence electron density transfer away from the C10 atom (due to electron delocalization between the amide and pyrrolidine moieties) destabilizes the corresponding C1s ionic state and hence increases C1s ionization energy. We also observed that the C1s band corresponding to C2 and C5 atoms in nitroxyl9 is narrower and has a higher ionization energy than in nitroxyl8. This can be attributed to hyperconjugative interactions ($\pi^* \leftarrow \sigma$ electron density transfer) between the C–CH_3 σ orbitals and the π^* orbital of the pyrrolidine ring. The depletion of electron density of C2 and C5 atoms increases their C1s ionization energies upon going from nitroxyl8 to nitroxyl9. Also, the C1s lifetimes of C2 and C5 core–holes will be increased which (according to the uncertainty principle) leads to reduced bandwidths mentioned above but the effect is probably too small (few meVs) to be observed with

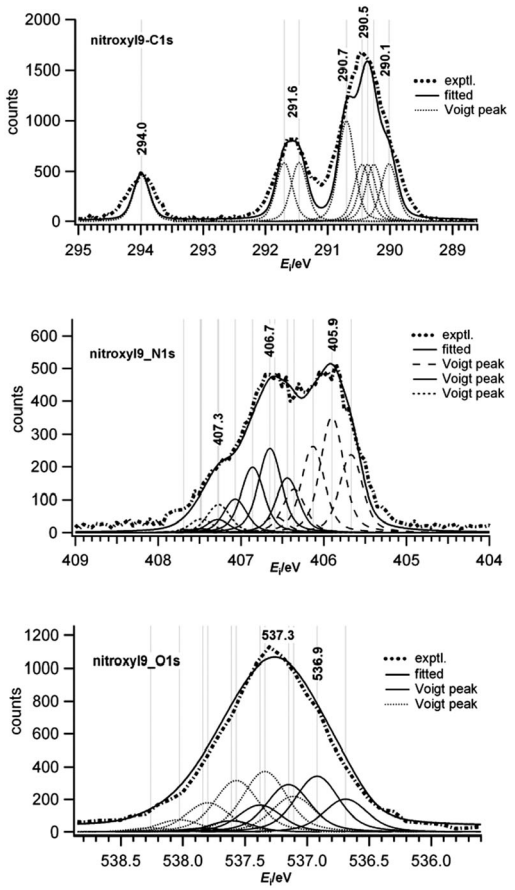

Fig. 7 C1s, N1s and O1s in XPS of the nitroxyl9 radical.

Table 2 Assignment of core ionizations in TEMPO, nitroxyl8 and nitroxyl9 (see Fig. 1 for atom labeling)

	E_i[a]/eV	C1s assignment	N1s assignment	O1s assignment
TEMPO	290.1	C7, C10		
	290.4	C8, C9, C5, C3		
	290.7	C4		
	291.3	C2, C6		
	406.4, 406.9		N	
	537.0			O
Nitroxyl8	290.1	C6, C7		
	290.4	C8, C9		
	290.7	C3, C4		
	291.4	C2, C5		
	293.8	C10		
	405.9		N1	
	406.4, 407.0		N2	
	536.8			O1
	537.2			O2
Nitroxyl9	290.1	C6		
	290.5	C8, C9, C7		
	290.7	C3, C4		
	291.6	C2, C5		
	294.0	C10		
	405.9		N1	
	406.7, 407.3		N2	
	536.9			O1
	537.3			O2

[a] Precision of the ionization energies is ±0.1 eV for all but C1s and shoulders in which it is ±0.2 eV.

the present resolution. Our XPS spectra reveal one more detail of the core electronic structure which supports the calculation results. The lowest energy C1s band in nitroxyl8 is broader than in nitroxyl9 with an additional shoulder appearing at 290.7 eV. The broadening may be attributed to the difference in the chemical environments of C3 and C4 atoms. While the chemical environments of C3 and C4 atoms differ in both nitroxyl8 and in nitroxyl9, the delocalization of π-electron density into amide moiety makes the C3 and C4 environments less different in the latter molecule. This can lead to a narrower corresponding C1s band in nitroxyl9.

The N1s spectral regions in nitroxyl8 and nitroxyl9 are much broader than in TEMPO and clearly indicate the presence of two types of nitrogen atoms in these molecules: amide and nitroxyl nitrogens. The partially resolved bands at 406.4 and 407.0 eV in nitroxyl8 and at 406.7 and 407.3 eV in nitroxyl9 can be attributed to nitroxyl nitrogens. This follows from comparison with the unsubstituted TEMPO molecule where the analogous bands appear at 406.4 and 406.9 eV. The amide group nitrogen is not bonded to the electronegative oxygen (as in the nitroxyl group) but to the much less electronegative carbon and hydrogen. It is not surprising therefore that amide N1s ionizations appear at lower ionization energies (405.9 eV) than nitroxyl N1s ionizations (Table 2). The N1s vibronic profile of both nitroxyls was fitted by Voigt functions (Fig. 6 and 7) assuming that vibrational progressions should be taken into consideration under the validity of the linear coupling model. For nitroxyl8 progression of 0.23 eV (dashed line) is suggested which is ascribed to amide N1s (S = 1.53), whereas in the presumed triplet–singlet split states (406.4, 407.0 eV) assigned to nitroxyl N1s a good fit achieved with ν = 0.21 eV, S = 1.53 (full line) and S = 0.49 (dotted line) respectively. The fitting of nitroxyl9 was performed with the same progressions (0.23 and 0.21 eV), with S = 1.49 for the amide nitrogen and S = 1.55 and 0.49 for the nitroxyl nitrogen (full line and dotted line, respectively).

The O1s spectral regions for nitroxyl8 and nitroxyl9 can be interpreted by using analogous arguments. The amide oxygen appears at a lower ionization energy than the nitroxyl oxygen as can be expected since the amide oxygen is bonded to the weakly electronegative carbon rather than to the more strongly electronegative nitrogen of the nitroxyl group. However, the energy separation between the amide and nitroxyl O1s bands is less pronounced than between the corresponding amide and nitroxyl N1s bands. This can again be rationalized by the fact that oxygen is more electronegative than nitrogen and holds electron density more tightly, which reduces chemical shifts induced by the molecular environment. According to the fitted spectra the amide oxygen is revealed just as a shoulder at 536.8 and 536.9 eV in nitroxyl8 and nitroxyl9 respectively. The maximum at 537.2 eV in nitroxyl8 and 537.3 eV in nitroxyl9 is assigned to nitroxyl O1s, but the multiplet splitting is not detected probably for the same reason.

Computational results

The ROHF ΔSCF predicted CEBEs are in good agreement with those of the experiment, in particular for the C atoms where no

Table 3 Core electron binding energies (in eV) calculated by the ROHF ΔSCF approach. The labeling of the atoms is in accordance with Fig. 1 and the numbers in italics are experimental values

	TEMPO	Nitroxyl8	Nitroxyl9
C2	291.37 *291.3*	291.70 *291.4*	291.88 *291.6*
C3	290.44 *290.4*	290.98 *290.7*	290.71 *290.7*
C4	290.50 *290.7*	291.05 *290.7*	290.72 *290.7*
C5	290.44 *290.4*	291.58 *291.4*	291.70 *291.6*
C6	291.37 *291.3*	290.34 *290.1*	290.30 *290.1*
C7	290.23 *290.1*	290.17 *290.1*	290.13 *290.5*
C8	290.30 *290.4*	290.60 *290.4*	290.62 *290.5*
C9	290.30 *290.4*	290.61 *290.4*	290.67 *290.5*
C10	290.23 *290.1*	294.77 *293.8*	294.91 *294.0*
N1	—	405.92 *405.9*	405.89 *405.9*
N2[a]	405.51 *406.4*	405.66 *406.4*	405.78 *406.7*
O1	—	536.10 *536.8*	536.14 *536.9*
O2[a]	535.65 *537.0*	540.69 *537.2*	538.50 *537.3*

[a] In TEMPO these atoms correspond to the N and O atoms (Fig. 1).

significant discrepancies are encountered (Table 3). The average absolute deviation from the experiment for the ROHF ΔSCF method is 0.47 eV. The C atoms vicinal to the electronegative N and O atoms have correspondingly larger CEBEs clearly distinguishable from the aliphatic C atoms (Table 3). Interestingly, although C1s CEBEs are expected to decrease with the increase in the C atom saturation, as observed *e.g.* in the C_2H_2, C_2H_4, C_2H_6 series,[5] and the vicinal amide group depletes the π density from C3 in nitroxyl9 *via* resonance effects, CEBE for the C3 atom is nevertheless predicted to be lower by 0.27 eV in nitroxyl9 relative to nitroxyl8. Thus, the core 1s orbital of the sp^3 hybridized C3 atom in nitroxyl8 exhibits much greater sensitivity to the electron withdrawing effects of the vicinal amide group. The highly electronegative atoms of the amide group also give rise to the lower CEBEs predicted for the CH_3 substituents located nearer to it (C6, C7 relative to C8, and C9). Overall, for the C1s ionizations, the accuracy achieved by the ROHF ΔSCF appears to be sufficient for a finer assignment of the experimental spectra providing more clues as to the detailed ordering of the C atoms signals within the compound bands. The results also give further support to the empirically derived band assignments given above.

On the other hand, some dubious ROHF ΔSCF results show up for the N and O core ionizations. In the case of the two N atoms of nitroxyl8 and nitroxyl9, they concern the predicted wrong ordering of the corresponding CEBEs. Namely, the CEBE for the amide N (N1) is expected to lie below that of the nitroxyl N (N2) because it is reasonable to assume that the value for the latter remains close to that measured in TEMPO (∼406–407 eV). The differences are minor though and reflect the subtle errors in the ROHF atomic charge densities due to the neglect of the correlation effects. This point is given further support upon considering the second-order perturbation correction for the correlation according to the recently calibrated ΔMP2 method.[5] The MP2 (specifically RMP) corrections are based on the present ROHF reference wave functions. It is found that, unlike the ΔSCF, the ΔMP2 method does predict the correct ordering of the CEBEs for the two N atoms in both nitroxyl8 and nitroxyl9. The ΔMP2 CEBEs for the N1 and N2 atoms of nitroxyl8 (nitroxyl9) equal 406.40 (406.32 eV) and 407.23 (407.28 eV), respectively. The relativistic corrections for the 1s core orbital in N and O atoms also gain in importance with the recent estimates amounting to +0.21 eV for N and +0.36 eV for O.[6] These should shift the two N CEBEs closer still to the observed band maxima so that the general agreement for the N core ionizations is good.

The largest discrepancy concerns the overestimated CEBEs for the O2 atoms, particularly that in nitroxyl8 (discrepancy >3 eV), which is thus effectively predicted to overlap with the O atom band of the CO_2 calibrant gas. This prediction was unambiguously shown to be erroneous upon performing the experiments without CO_2, which revealed that no peak was hidden underneath the O signal of CO_2. Interestingly, in TEMPO no such error is observed and the O CEBE, especially if the relativistic correction is taken into account,[6] draws much closer to the observed 537 eV value (Tables 2 and 3). Still, the errors are significantly larger than those typically seen in the case of the O atoms of ground state closed shell species,[5,6] and illustrate the extra difficulties presented with the open shell species, in particular considering that the O2 atom formally acts as the radical center in these molecules. Namely, it is found that the 2p orbital of O2 has a larger contribution than the 2p orbital of N2 to the π*(N–O) singly occupied molecular orbital, *i.e.* the unpaired spin density is shifted closer to O2, which is also in line with the observed spectral features (*vide ante*). Another discrepancy is in the large predicted differences in the O2 CEBEs (>2 eV, Table 3) of the closely analogous nitroxyl8 and nitroxyl9, which are clearly unphysical because they cannot be traced to any significant differences in their ground state properties. Specifically, we found no significant differences between the nitroxyl8 and nitroxyl9 ground states with regards to the N–O bond lengths, Mulliken (or Löwdin) atomic charges, and O2 1s orbital energies. Thus, these errors are likely an indication of instabilities in the ROHF core–hole wave function, specifically the emergence of close-lying SCF minima when the complexity of the molecule is increased

through the introduction of the amide functional groups in nitroxyl8 and nitroxyl9. Although demonstrating this point unambiguously by pushing an already converged core–hole state to another, a slightly lower minimum is difficult to achieve systematically, we managed to obtain two such ROHF minima giving rise to $\sim$1 eV different CEBEs in the case of the N2 atom of nitroxyl8, which is indicative at the least. Thus, generally radical centers and probably also the atoms adjacent to them appear more prone to errors in the ROHF ΔSCF approach to calculating CEBEs.

Conclusion

We have measured the photoionization spectra of three stable nitroxyl radicals in the VUV and X-ray regions. Our most important results indicate that the unpaired electron in the nitroxyl group is located closer to the oxygen than to the nitrogen atom and that amide substitution perceptibly changes core ionization energies as evidenced by the splitting and broadening of N1s and O1s bands. The linear coupling model (LCM) applied for their spectral analysis helped us to assign different bands more reliably using the vibrational modes that might contribute to the vibrational progressions in the particular ionic states. In most of them $I(1 \leftarrow 0)$ transition was the most intense one indicating the change of geometry within the FC zone. Since the vibrational structure of the spectra of these rather complex molecules were not resolved because of the limits in the instrumental resolution and many vibrations that accompany the ionizations, we were primarily interested in predicting the FC envelopes. In the analysis of the C1s spectra of the three nitroxyl radicals we decided to limit the deconvolution procedure to just one Voigt profile per C atom to avoid arbitrariness in choosing one out of many vibrational modes that could be responsible for the vibronic progressions of approximately 0.2 eV. TEMPO C1s was an exception for which we resorted to a sort of 'hybrid' approach in that we used the LCM arguments for the band at 291.3 eV thus achieving a very good fit of the C1s spectra.

The three open-shell molecules also provided an unusually difficult test case for the assessment of the reliability of the ROHF based ΔSCF method used to predict the core electron binding energies. In summary, the agreement between the predictions and the experiment was found to be best for the C1s and somewhat poorer for the O1s and N1s core ionizations, in particular for the N and O atoms of the nitroxyl radical center.

The UPS and XPS results reported here could both be useful in different areas of research pertaining to SNR. SNR are known to form intermolecular hydrogen bonds as established by IR and ESR spectroscopy.[22] The XPS method can also possibly detect such bonds in the solid state, but in that case the knowledge of core energy levels (from XPS data) is essential. Furthermore, SNR act as chelating ligands to metals[23] utilizing the unpaired electron in the π^* orbital. When studying bonding in these coordination complexes, UPS data on SNR valence energy levels can be useful, for instance, in predicting relative chelating abilities of various SNR ligands. Our high-resolution UPS and XPS results can also provide information useful in studies of chemisorption and reaction mechanisms of SNR on metal surfaces, for example, similar to the work reported by Katter *et al.*[24] Once again accurate information about both valence and core orbital energies in free SNR and their ions is essential for such studies.[25]

Acknowledgements

I.N. thanks the Faculty of Science, Charles Sturt University for the financial support of this work through the Seed Grant A105-954-639-3495. B.K. and I.Lj. thank the Ministry of Science, Education and Sports of the Republic of Croatia for the financial support through Projects 098-0982915-2945 and 098-0982915-2944. The research leading to these results has received funding from the European Community's Seventh Framework Programme (FP7/2007–2013) under grant agreement no. 312284.

Notes and references

1 (*a*) K. Hideg, T. Kalai and C. P. Sar, *J. Heterocycl. Chem.*, 2005, **42**, 437; (*b*) M. T. Lemaire, *Pure Appl. Chem.*, 2004, **76**, 277; (*c*) R. G. Hicks, *Org. Biomol. Chem.*, 2007, **5**, 1321; (*d*) T. Eliash, A. Barbon, M. Brustolon, M. Sheves, I. Bilkis and L. Weiner, *Angew. Chem., Int. Ed.*, 2013, **52**, 8689.

2 I. Novak, L. J. Harrison, B. Kovač and L. M. Pratt, *J. Org. Chem.*, 2004, **69**, 7628 and references cited therein.

3 (*a*) V. S. Sastri, M. Elboujdaini, J. R. Perumareddi and J. R. Brown, *Appl. Surf. Sci.*, 1996, **93**, 31; (*b*) L. N. Mazalov, A. D. Fedorenko, V. I. Ovcharenko, E. V. Tretyakov, E. Yu Fursova and N. A. Kryuchkova, *J. Struct. Chem.*, 2011, **52**, S102.

4 (*a*) D. W. Davis, R. L. Martin, M. S. Banna and D. A. Shirley, *J. Chem. Phys.*, 1973, **59**, 4235; (*b*) K. J. Børve and T. D. Thomas, *J. Chem. Phys.*, 1999, **111**, 4478; (*c*) A. Rüdel, U. Hergenhahn, K. Maier, E. E. Rennie, O. Kugeler, J. Viefhaus, P. Lin, R. R. Lucchese and A. M. Bradshaw, *New J. Phys.*, 2005, **7**, 18.

5 J. Shim, M. Klobukowski, M. Barysz and J. Leszczynski, *Phys. Chem. Chem. Phys.*, 2011, **13**, 5703.

6 N. A. Besley, A. T. B. Gilbert and P. M. W. Gill, *J. Chem. Phys.*, 2009, **130**, 124308.

7 K. C. Prince, R. R. Blyth, R. Delaunay, M. Zitnik, J. Krempasky, J. Slezak, R. Camilloni, L. Avaldi, M. Coreno, G. Stefani, C. Furlani, M. de Simone and S. Stranges, *J. Synchrotron Radiat.*, 1998, **5**, 565.

8 W. L. Jolly, K. D. Bomben and C. J. Eyermann, *At. Data Nucl. Data Tables*, 1984, **31**, 433.

9 D. E. Woon and T. H. Dunning, Jr., *J. Chem. Phys.*, 1995, **103**, 4572.

10 T. H. Dunning Jr., *J. Chem. Phys.*, 1989, **90**, 1007.

11 E. Miyoshi, H. Mori, R. Hirayama, Y. Osanai, T. Noro, H. Honda and M. Klobukowski, *J. Chem. Phys.*, 2005, **122**, 074104.
12 P. Pulay, *J. Comput. Chem.*, 1982, **3**, 556.
13 M. W. Schmidt, K. K. Baldridge, J. A. Boatz, S. T. Elbert, M. S. Gordon, J. J. Jensen, S. Koseki, N. Matsunaga, K. A. Nguyen, S. Su, T. L. Windus, M. Dupuis and J. A. Montgomery, *J. Comput. Chem.*, 1993, **14**, 1347.
14 (*a*) W. Turley and F. P. Boer, *Acta Crystallogr., Sect. B: Struct. Crystallogr. Cryst. Chem.*, 1972, **28**, 1641; (*b*) P. B. Chion and J. Lajzerowicz, *Acta Crystallogr., Sect. B: Struct. Crystallogr. Cryst. Chem.*, 1975, **31**, 1430; (*c*) Z. Ciunik, *J. Mol. Struct.*, 1997, **412**, 27.
15 J. J. Yeh, *Atomic Calculation of Photoionization Cross-sections and Asymmetry Parameters*, Gordon and Breach, Langhorne, PA, 1993.
16 (*a*) C. Nicolas and C. Miron, *J. Electron Spectrosc. Relat. Phenom.*, 2012, **185**, 267; (*b*) L. Rintoul, A. S. Micallef and S. E. Bottle, *Spectrochim. Acta, Part A*, 2008, **70**, 713.
17 (*a*) W. Domcke, L. S. Cederbaum, H. Köppel and W. von Niessen, *Mol. Phys.*, 1977, **34**, 1759; (*b*) S. J. Osborne, S. Sundin, A. Ausmees, S. Svensson, L. J. Saethre, O. Svaeren, S. L. Sorensen, J. Végh, J. Karvonen, S. Aksela and A. Kikas, *J. Chem. Phys.*, 1997, **106**, 1661; (*c*) L. J. Sæthre, O. Sværen, S. Svensson, S. Osborne and T. D. Thomas, *Phys. Rev. A: At., Mol., Opt. Phys.*, 1997, **55**, 2748.
18 J. Lalevee, X. Allonas and P. Jacques, *THEOCHEM*, 2006, **767**, 143.
19 E. E. Rennie, U. Hergenhahn, O. Kugeler, A. Rüdel, S. Marburger and A. M. Bradshaw, *J. Chem. Phys.*, 2002, **117**, 6524.
20 B. Kempgens, K. Maier, A. Kivimäki, H. M. Köppe, M. Neeb, M. N. Piancastelli, U. Hergenhahn and A. M. Bradshaw, *J. Phys. B: At. Mol. Phys.*, 1997, **30**, L741.
21 A. Greenberg, T. D. Thomas, C. R. Bevilacqua, M. Coville, D. Ji, J.-C. Tsai and G. Wu, *J. Org. Chem.*, 1992, **57**, 7093.
22 P. Franchi, M. Lucarini, P. Pedrielli and G. F. Pedulli, *ChemPhysChem*, 2002, **3**, 789.
23 M. T. Lemaire, *Pure Appl. Chem.*, 2004, **76**, 277.
24 U. J. Katter, T. Hill, T. Risse, H. Schlienz, M. Beckendorf, T. Klulner, H. Hamann and H.-J. Freund, *J. Phys. Chem. B*, 1997, **101**, 552.
25 D. Kubala, K. Regeta, R. Janečkova, J. Fedor, S. Grimme, A. Hansen, P. Nesvadba and M. Allan, *Mol. Phys.*, 2013, **111**, 2033.

